Journal of Organometallic Chemistry 905 (2020) 121021

Contents lists available at ScienceDirect

Journal of Organometallic Chemistry

journal homepage: www.elsevier.com/locate/jorganchem

Oxidation reactions, coordination chemistry and antibacterial activities with ligand 2-{(diphenylphosphino)methyl}-*N,N*-dimethylaniline

Harbi Tomah Al-Masri

Department of Chemistry, Faculty of Sciences, Al al-Bayt University, P.O. Box 130040, Mafraq, 25113, Jordan

ARTICLE INFO

Article history:
Received 4 November 2019
Accepted 6 November 2019
Available online 7 November 2019

Keywords:
Sulfur
Selenium
Tungsten
Molybdenum
Antibacterial
Copper

ABSTRACT

N,N-dimethyl-*o*-toluidine was treated with *n*-butyllithium-tmeda in diethylether/hexane solution to give (2-(dimethylamino)benzyl)lithium which reacts with chlorodiphenylphosphine to form the corresponding hemilabile *N,P*-ligand 2-PPh_2CH_2-1-$NMe_2C_6H_4$ (**1**). Oxidation of **1** with elemental sulfur or gray selenium gave the corresponding sulfide and selenide 2-(E)PPh_2CH_2-1-$NMe_2C_6H_4$ (E = S (**2**), Se (**3**)), respectively. The reaction of **1** with $M(CO)_6$ (M = Mo, W) afforded *cis*-$[Mo(CO)_4\{2\text{-}PPh_2CH_2\text{-}1\text{-}NMe_2C_6H_4\}_2]$(**4**) and *trans*-$[W(CO)_4\{2\text{-}PPh_2CH_2\text{-}1\text{-}NMe_2C_6H_4\}_2]$(**5**), respectively. The treatment of **1** with copper(I) iodide in 1:1 mol ratio produced $[CuI\{2\text{-}PPh_2CH_2\text{-}1\text{-}NMe_2C_6H_4\}]_2$ (**6**). The complexes **4**–**6** have been screened for antibacterial activity and the results were compared with the activity of the free ligand **1** against four bacterial strains. Complexes **4** and **6** had the highest antibacterial activity and can be considered as promising antimicrobial agents. Compounds **1**–**6** were characterized by multinuclear NMR spectroscopy (^1H, ^{13}C, ^{31}P, ^{77}Se NMR), IR and elemental analysis. Crystal structure determinations of **1**, **2**, **4**, and **6** were carried out.

1. Introduction

The importance of bidentate ligands with '*soft*' and '*hard*' donor atoms in homogenous catalysis for industrially important reactions, coordination chemistry and medicinal chemistry has been the subject of review papers [1]. The ^2_K–*P,N* ligands chosen are known to exhibit hemilability, whereby at least one of the donors is strongly coordinating and anchored to the metal, while the more labile donor(s) can be displaced by catalytic substrates [2]. A number of complexes of Rh [2–6], Ir [7,8], Ru [9–12], Pd, Pt [13,14] and Re [15] containing bidentates Ph_2P, Me_2N-donor ligands with aromatic backbone have been described. However, no examples of such ligands with group 6 metal carbonyls which contain a six- or a seven-membered chelate ring have been reported to date. Only a few related examples of the type $[M(CO)_4\{2\text{-}PPh_2\text{-}1\text{-}NMe_2C_6H_4\}]$ (M = Mo, W) with a five-membered chelate ring have been reported [16].

We previously reported the synthesis and the structurally characterized ^2_K–*N,N*- or ^2_K–*O,N*-ligands bearing Me_2N arm [17], as these are useful starting materials for main group and transition metal complexes in which they act as ^2_K–*N,N*- or ^2_K–*O,N*-chelating ligands forming six- and seven-membered chelate rings [18].

We now report the synthesis, spectroscopic properties of 2-PPh_2CH_2-1-$NMe_2C_6H_4$ (**1**), 2-(E)PPh_2CH_2-1-$NMe_2C_6H_4$ (E = S (**2**), Se (**3**)), *cis*-$[Mo(CO)_4\{2\text{-}PPh_2CH_2\text{-}1\text{-}NMe_2C_6H_4\}_2]$(**4**), *trans*-$[W(CO)_4\{2\text{-}PPh_2CH_2\text{-}1\text{-}NMe_2C_6H_4\}_2]$(**5**) and $[CuI\{2\text{-}PPh_2CH_2\text{-}1\text{-}NMe_2C_6H_4\}]_2$ (**6**). The structures of **1**, **2**, **4** and **6** have been determined by X-ray crystallography.

2. Experimental section

2.1. General remarks

All experiments were carried out under purified dry nitrogen using standard *Schlenk* and vacuum line techniques. Solvents were dried and freshly distilled under nitrogen [19]. The chemicals $Mo(CO)_6$, $W(CO)_6$, CuI, *n*-BuLi, and *N,N*-dimethyl-*o*-toluidine were used as purchased. Infrared spectra were recorded with a PerkinElmer System 2000 FT-IR spectrometer between 4000 and 400 cm^{-1} using KBr disk. The NMR spectra were recorded at 25 °C on a Bruker AVANC DRX 400 MHz spectrometer operating at

E-mail address: harbialmasri@yahoo.com.

https://doi.org/10.1016/j.jorganchem.2019.121021
0022-328X/

400.17 MHz (^{1}H), 100.63 MHz (^{13}C), 161.99 MHz (^{31}P) and 76.36 MHz (^{77}Se) using tetramethylsilane for ^{1}H and ^{13}C, 85% H_3PO_4 for ^{31}P and Me_2Se for ^{77}Se NMR as external standards. For **2** and **6** the NMR spectra were recorded at 25 °C on a Bruker AVANC DRX 300 MHz spectrometer operating at 300.13 MHz (^{1}H), 75.47 MHz (^{13}C). Microanalyses were performed on a Flash 2000 elemental analyzer. Melting points were carried out with Gallenkamp Model apparatus with open capillaries.

The antimicrobial activity of selected complexes was evaluated using four bacterial strains; two Gram positive (*Bacillus subtillis* (NCTC-1040) and *Staphylococcus aureus* (NCTC-7447) and two Gram negative (*Escherichia coli* (NCTC-10416) and *Salmonella typhi* (NCIMB-9331) bacteria. Bacterial cultures were provided by the microbiology lab at Al al-Bayt University. Each bacterial strain was subcultured on nutrient agar medium (Merck, Germany) and incubated overnight at 37 °C. Disc diffusion method was used to evaluate the antibacterial activity of each complex. Sterile Matricel (BBL, cocksville USA) 6.0 mm filter paper discs were impregnated with 1 mg/ml of each test complex and dried to evaporate the residual solvent (dimethyl sulfoxide (DMSO)). Imipenem was used as positive control to ensure the activity of standard antibiotic against the test organisms. The sample discs, the standard antibiotic discs, and dried blank disc impregnated with DMSO (negative control) were placed gently on previously marked zones in the agar plates pre-inoculated with the test bacteria. The plates were then kept in a refrigerator at 4 °C for about 24 h upside down to allow sufficient diffusion of the materials from the discs to the surrounding agar medium. The plates were then inverted and kept in an incubator at 37 °C for 24 h. After incubation, the antimicrobial activity of the test complexes was determined by measuring the diameter of the inhibition zone around the disc.

2.2. Preparation of 1–6

2.2.1. 2-{(diphenylphosphino)methyl}-N,N-dimethylaniline (1)

A solution of 2.5 M *n*-BuLi in *n*-hexane (45.6 ml, 0.114 mol) was added dropwise to a well-stirred solution containing *N,N*-dimethyl-*o*-toludiene (15 g, 0.114 mol) and *N,N,N′,N′*-tetramethylethylenediamine (8.61 ml, 0.06 mol) in *n*-hexane (100 mL). The resulting yellow solution was stirred for 3 h at room temperature, after that PPh_2Cl (25.15 g, 0.114 mol) in diethylether (100 mL) was added dropwise at −4 °C (salted ice bath). The mixture was then allowed to reach room temperature and stirred for 2 h. After this time, ethanol (5 mL) and water (100 mL) were added to quench the reaction and the product was extracted with ether (3 × 50 mL) and dried over sodium sulfate. The solvent was removed under reduced pressure and the viscous residue was recrystallized from a *n*-hexane/ethanol solution to give the product as colorless crystals in 85% yield. Mp 82–84 °C. **^{1}H NMR** ($CDCl_3$, δ/ppm): 2.65 (s, 6H, $N(CH_3)_2$), 3.58 (br., 2H, CH_2), 6.89–7.50 (m, 14H, C_6H_4 and C_6H_5). **^{13}C NMR** ($CDCl_3$, δ/ppm): 30.2 (d, $^{1}J_{C\text{-}P}$ = 15.1 Hz, CH_2), 45.1 (s, $N(CH_3)_2$), 119.9 (s), 123.3 (d, $J_{C\text{-}P}$ = 1.5 Hz), 126.7 (d, $J_{C\text{-}P}$ = 2.0 Hz), 128.2 (d, $J_{C\text{-}P}$ = 7.1 Hz), 128.4 (s), 130.5 (d, $J_{C\text{-}P}$ = 11.0 Hz), 132.9 (d, $J_{C\text{-}P}$ = 18.2 Hz), 133.11 (d, $J_{C\text{-}P}$ = 7.0 Hz), 139.1 (d, $J_{C\text{-}P}$ = 16.1 Hz), 152.9 (d, $J_{C\text{-}P}$ = 4.0 Hz),. **^{31}P** NMR ($CDCl_3$, δ/ppm): 9.46 (s, 1P). **IR** (KBr, cm^{-1}): ύ = 1433 s, 1097s, 923 m, 748 m, 696 s, 576 s. Anal. calcd. for $C_{21}H_{22}NP$: C 78.97; H 6.94; N 4.39%. Found: C 78.95; H 6.93; N 4.40%.

2.2.2. 2-{(diphenylphosphinothioyl}methyl)-N,N-dimethylaniline (2)

A mixture of **1** (1.00 g, 3.13 mmol) and elemental sulfur (0.10 g, 3.13 mmol) in dry toluene (50 mL) was refluxed for 4 h. The solution was filtered through Celite while hot and the solvent was reduced to 10 mL and kept at room temperature to afford off-white crystals of **2** in 65% yield. Mp 83–85 °C. **^{1}H NMR** ($CDCl_3$, δ/ppm): 2.31 (s, 6H, $N(CH_3)_2$), 4.01 (d, $^{3}J_{H\text{-}H}$ = 14.4 Hz, 2H, CH_2), 6.86–7.69 (m, 14H, C_6H_4 and C_6H_5). **^{13}C NMR** ($CDCl_3$, δ/ppm): 34.7 (d, $^{1}J_{C\text{-}P}$ = 51.85 Hz, CH_2), 45.3 (s, $N(CH_3)_2$), 120.3 (d, $J_{C\text{-}P}$ = 2.8 Hz), 123.8 (d, $J_{C\text{-}P}$ = 2.9 Hz), 127.4 (d, $J_{C\text{-}P}$ = 6.6 Hz), 128.2 (d, $J_{C\text{-}P}$ = 2.9 Hz), 128.3 (d, $J_{C\text{-}P}$ = 5.7 Hz), 131.2 (d, $J_{C\text{-}P}$ = 1.7 Hz), 131.4 (d, $J_{C\text{-}P}$ = 23.9 Hz), 132.1 (d, $J_{C\text{-}P}$ = 48.4 Hz), 133.4 (s), 153.2 (d, $J_{C\text{-}P}$ = 6.3 Hz). **^{31}P NMR** ($CDCl_3$, δ/ppm): 44.79 (s, 1P). **IR** (KBr, cm^{-1}): ύ = 1489 s, 1433 s, 1303 m, 1043 s, 650 s. Anal. calcd. for $C_{21}H_{22}NPS$: C 71.77; H 6.31; N 3.99%. Found: C 71.78; H 6.31; N 4.10%.

2.2.3. 2-{(diphenylphosphinoselenoyl)methyl}-N,N-dimethylaniline (3)

Compound **3** was synthesized as for **2** by using gray selenium (0.25 g, 3.13 mmol) instead of elemental sulfur and colorless crystals were obtained in 75% yield. Mp 125–127 °C. **^{1}H NMR** ($CDCl_3$, δ/ppm): 2.91 (s, 6H, $N(CH_3)_2$), 4.53 (d, $^{3}J_{H\text{-}H}$ = 13.21 Hz, 2H, CH_2), 7.02–8.06 (m, 14H, C_6H_4 and C_6H_5). **^{13}C NMR** ($CDCl_3$, δ/ppm): 35.0 (d, $^{1}J_{C\text{-}P}$ = 45.3 Hz, CH_2), 45.1 (s, $N(CH_3)_2$), 120.3 (d, $J_{C\text{-}P}$ = 4.0 Hz), 123.7 (d, $J_{C\text{-}P}$ = 3.0 Hz), 127.4 (d, $J_{C\text{-}P}$ = 4.04 Hz), 128.2 (d, $J_{C\text{-}P}$ = 12.1 Hz), 128.3 (d, $J_{C\text{-}P}$ = 4.0 Hz), 128.5 (d, $J_{C\text{-}P}$ = 12.1 Hz), 131.1 (d, $J_{C\text{-}P}$ = 5.0 Hz), 131.2 (d, $J_{C\text{-}P}$ = 3.0 Hz), 132.2 (d, $J_{C\text{-}P}$ = 9.1 Hz), 153.2 (d, $J_{C\text{-}P}$ = 7.1 Hz). **^{31}P NMR** ($CDCl_3$, δ/ppm): 34.93 (s, 1P, $^{1}J_{Se-P}$ = 725.7 Hz). **^{77}Se NMR** ($CDCl_3$, δ/ppm): 286.53 (d, 1Se, $^{1}J_{Se-P}$ = 729.6 Hz). **IR** (KBr, cm^{-1}): ύ = 1429 s, 1433 s, 1296 s, 1095 s, 945 m, 756 m, 695 s, 526 s. Anal. calcd. for $C_{21}H_{22}NPSe$: C 63.32; H 5.57; N 3.52%. Found: C 63.40; H 5.53; N 3.48%.

2.2.4. cis-Tetracarbonylbis{2-[(diphenylphosphino-$_K$P)methyl)]-N,N-dimethylaniline}molybdenum (0) (4)

A mixture of compound **1** (1.00 g, 3.13 mmol) and $Mo(CO)_6$ (0.80 g, 3.13 mmol) in *n*-hexane (80 mL) was refluxed for 12 h to give a dark brown solution. Solvent was reduced to 10 mL under reduced pressure. Cooling this solution to 4 °C gave **4** as yellow crystals in 80% yield. Mp 150–152 °C. **^{1}H NMR** ($CDCl_3$, δ/ppm): 2.17 (s, 6H, $N(CH_3)_2$), 3.70 (br., 2H, CH_2), 6.48–7.20 (m, 14H, C_6H_4 and C_6H_5). **^{13}C NMR** ($CDCl_3$, δ/ppm): 34.16 (t, $^{1}J_{C\text{-}P}$ = 8.05 Hz, CH_2), 44.71 (s, $N(CH_3)_2$), 119.6 (s), 122.9 (s), 127.1 (s), 127.6 (t, $J_{C\text{-}P}$ = 4.0 Hz), 128.9 (s), 131.0 (t, $J_{C\text{-}P}$ = 3.0 Hz), 131.1 (t, $J_{C\text{-}P}$ = 6.1 Hz), 135.4 (t, $J_{C\text{-}P}$ = 14.1 Hz), 135.6 (d, $J_{C\text{-}P}$ = 14.1 Hz), 153.2 (s), 209.8 (t, $^{2}J_{C\text{-}P}$ = 9.1 Hz, C≡O_{eq}), 216.4 (t, $^{2}J_{C\text{-}P}$ = 8.1 Hz, C≡O_{ax}). **^{31}P NMR** ($CDCl_3$, δ/ppm): 34.96 (s, 1P). **IR** (KBr, cm^{-1}): ύ = 1925 vs, 1861 vs (C≡O), 1431 s, 1092 m, 692 s, 584 m. Anal. calcd. for $C_{46}H_{44}N_2P_2MoO_4$: C 65.25; H 5.24; N 3.31%. Found: C 65.23; H 5.27; N 3.33%.

2.2.5. trans-Tetracarbonylbis{2-[(diphenylphosphino-$_K$P)methyl)]-N,N-dimethylaniline}tungsten(0) (5)

A mixture of compound **1** (1.00 g, 3.13 mmol) and $W(CO)_6$ (1.10 g, 3.13 mmol) in *n*-hexane (80 mL) was refluxed for 16 h to give a dark brown solution. Solvent was removed under reduced pressure and the product extracted into ethanol (15 mL). Cooling this solution to 4 °C gave **5** as yellow crystals in 65% yield. Mp 210–212 °C. **^{1}H NMR** ($CDCl_3$, δ/ppm): 2.31 (s, 6H, $N(CH_3)_2$), 4.08 (br., 2H, CH_2), 6.64–7.42 (m, 14H, C_6H_4 and C_6H_5). **^{13}C NMR** ($CDCl_3$, δ/ppm): 36.0 (t, $^{1}J_{C\text{-}P}$ = 10.1 Hz, CH_2), 44.8 (s, $N(CH_3)_2$), 119.6 (s), 122.9 (s), 127.1 (s), 127.6 (t, $J_{C\text{-}P}$ = 4.0 Hz), 128.9 (s), 130.4 (s), 132.7 (t, $J_{C\text{-}P}$ = 6.0 Hz), 133.2 (t, $J_{C\text{-}P}$ = 6.0 Hz), 138.2 (t, $J_{C\text{-}P}$ = 19.1 Hz), 153.4 (s), 203.4 (t, $^{2}J_{C\text{-}P}$ = 6.0 Hz, 4C≡O). **^{31}P NMR** ($CDCl_3$, δ/ppm): 22.08 (s, 1P, $^{1}J_{W-P}$ = 278.6 Hz). **IR** (KBr, cm^{-1}): ύ = 1863 vs (C≡O), 1491 s, 1431 s, 1090 m, 696 s, 615 s, 582 m. Anal. calcd. for $C_{46}H_{44}N_2P_2WO_4$: C 59.11; H 4.74; N 3.0%. Found: C 59.12; H 4.72; N 3.11%.

2.2.6. Di-μ-iodobis{2-[(diphenylphosphino-$_K$P)methyl)]-N,N-dimethylaniline-$_K$N}di-copper (6)

A mixture of CuI (0.60 g, 0.42 mmol) and ligand **1** (1.00 g,

3.13 mmol) in acetonitrile (70 mL) was stirred at room temperature for 5 h. The reaction solution was evaporated under vacuum and the desired complex was obtained as white solids. Recrystallization from dichloromethane/*n*-hexane gave complex **1** as colorless crystals in 70% yield. Mp 207–209 °C. **^{1}H NMR** ($CDCl_3$, δ/ppm): 2.86 (s, 12H, $N(CH_3)_2$), 3.68 (br., 4H, CH_2), 6.77–7.56 (m, 28H, C_6H_4 and C_6H_5). **^{13}C NMR** ($CDCl_3$, δ/ppm): 33.0 (s, CH_2), 47.2 (s, $N(CH_3)_2$), 119.1 (s), 123.6 (s), 127.7 (s), 128.0 (d, $J_{C\text{-}P} = 23.6$ Hz), 128.3 (s), 129.7 (s), 132.5 (s), 132.7 (s), 133.5 (d, $J_{C\text{-}P} = 13.5$ Hz), 152.3 (s). **^{31}P NMR** ($CDCl_3$, δ/ppm): 32.87 (s, 1P). **IR** (KBr, cm^{-1}): ύ = 1489 s, 1437 s, 1097 m, 695 s, 582 m. Anal. calcd. for $C_{42}H_{44}N_2P_2Cu_2$: C 65.87; H 5.79; N 3.66%. Found: C 65.80; H 5.74; N 3.64%.

2.3. Data collection and structure determination

Crystallographic data are given in Table 1. Single-crystal X-ray diffraction data were collected using $Mo_{K\alpha}$ radiation ($\lambda = 0.71073$ Å) on an Xcalibur-Eos-Gemini diffractometer. Crystals were maintained at 293K during data collection. Using Olex2 [20], The structures were solved with the ShelXT [21] structure solution program using Intrinsic Phasing and refined with the ShelXL [21] refinement package using Least Squares minimization. The Crystallographic data (excluding structure factors) have been deposited with the Cambridge Crystallographic Data Centre, CCDC, 12 Union Road, Cambridge CB21EZ, UK. Copies of the data can be obtained free of charge on quoting the depository numbers CCDC-**1952201** for **1,** CCDC-**1952202** for **2**, CCDC-**1952203** for **4** and CCDC-**1952204** for **6** (Fax: +44-1223-336-033; E-Mail: deposit@ccdc.cam.ac.uk, http://www.ccdc.cam.ac.uk).

3. Results and discussion

3.1. Synthesis

N,N-dimethyl-*o*-toluidine was treated with *n*-butyllithium-tmeda in ether/hexane solution for 2–3 h to afford the (2-(dimethylamino)benzyl)lithium intermediate which was further reacted with PPh_2Cl compound to give the corresponding 2-((diphenylphosphino)methyl)-*N,N*-dimethylaniline (**1**). This compound was previously synthesized without disclosure of spectral data [22a] according to reported procedure for 2-PPh_2-1-$NMe_2CH_2C_6H_4$ ligand [22b]. In this study the ligand was synthesized by a modified version of a literature method [22b] and fully characterized by multinuclear NMR spectroscopy, IR, elemental analysis and single crystal X-ray diffraction. The oxidation reaction of **1** with elemental sulfur or gray selenium in toluene gives the corresponding sulfide **2** and selenide **3**, respectively, as illustrated in Scheme 1.

The reaction of ligand **1** with $M(CO)_6$ (M = Mo, W) under reflux in *n*-hexane afforded *cis*-[$Mo(CO)_4${2-PPh_2CH_2-1-$NMe_2C_6H_4$ }$_2$] (**4**) and *trans*-[$W(CO)_4${2-PPh_2CH_2-1-$NMe_2C_6H_4$ }](**5**). Moreover, The treatment of **1** with cuprous iodide in 1:1 mol ratio afforded [CuI{2-PPh_2CH_2-1-$NMe_2C_6H_4$ }]$_2$ (**6**) (Scheme 1).

Compounds **1**–**6** were isolated and fully characterized by multinuclear NMR spectroscopy, IR and elemental analysis. Furthermore, the molecular structures of **1**, **2**, **4**, and **6** were elucidated by single crystal X-ray diffraction.

3.2. ^{1}H, ^{13}C, ^{31}P, ^{77}Se NMR and IR spectra

In the ^{1}H NMR spectrum, the most noticeable resonance is that due to the $N(CH_3)_2$ protons, which show a singlet for each compounds at 2.65 (**1**), 2.31 (**2**), 2.91 (**3**), 2.17 (**4**), 2.31 (**5**) and 2.68 ppm (**6**). The resonances corresponding to the benzylic protons are observed as broad singlets (3.58 (**1**), 3.70 (**4**), 4.08 (**5**)), doublets (4.01 (**2**), 4.53 (**3**)) and a well resolved singlet (3.68 (**6**)).

The ^{13}C NMR spectra of **1**–**6** reveal the resonances of the $N(CH_3)_2$ carbon atoms which exhibit resonances at 45.1 (**1**), 45.3 (**2**), 45.1 (**3**), 44.7 (**4**), 44.8 (**5**) and 47.2 ppm (**6**). Moreover, the resonances corresponding to the methylene carbon atoms are observed at 30.2 (**1**), 34.7 (**2**), 35.0 (**3**) as doublets, 34.2 (**4**), 36.0 (**5**) as triplets and 33.0 (**6**) as singlet. The ^{1}H NMR (6.48–7.78 ppm) and ^{13}C NMR (119.1–153.8 ppm) signals of the phenyl groups are in the expected range.

Interestingly, in **4** and **5**, the ligand behaves as $_\kappa P$-coordination mode rather than $^2_\kappa P,N$-mode. The non-occurrence of $^2_\kappa P,N$-mode is unambigously due to reaction condition, and may be obtained if the reaction is carried out at higher temperatures and for longer time. It is interesting that intramolecular binding of the ammine is clearly

Table 1
Crystal data and structure refinement for **1**, **2**, **4** and **6**.

	1	2	4	6
Formula	$C_{42}H_{44}N_2P_2$	$C_{21}H_{22}NPS$	$C_{46}H_{44}MoN_2O_4P_2$	$C_{42}H_{44}Cu_2I_2N_2P_2$
M_r	638.73	351.42	846.71	1019.61
Temp [K]	293(2)	293(2)	293(2)	293(2)
Crystal system	monoclinic	monoclinic	triclinic	monoclinic
Space group	$P\,2_1/c$	$P\,2_1/n$	$P\,\bar{1}$	$P\,2_1$
a [Å]	20.6885(11)	9.5400(4)	9.3720(5)	10.3547(8)
b [Å]	9.1084(6)	14.2269(5)	10.6896(5)	12.5513(6)
c [Å]	19.7458(12)	14.0999(4)	22.8077(11)	16.3110(9)
α [°]	90	90	87.189(4)	90
β [°]	105.199(6)	97.268(3)	89.573(4)	107.327(7)
γ [°]	90	90	73.394(5)	90
V [Å^3]	3590.7(4)	1898.33(12)	2187.0(2)	2023.7(2)
Z	4	4	2	2
ρ_{calcd} (Mg m^{-3})	1.182	1.230	1.286	1.673
$F(000)$	1360	744	876	1008
Abs coeff (mm^{-1})	0.153	0.256	0.416	2.687
No. of rflns coll.	17246	17417	19261	17903
No. of indep rflns	8312	4659	10108	9353
R_{int}	0.0236	0.0263	0.0292	0.0228
No. of parameters	415	217	497	452
R_1 ($I > 2\sigma(I)$)	0.0498	0.0430	0.0429	0.0306
wR_2 (all data)	0.1331	0.1128	0.0948	0.0693
$(\Delta/\rho)_{max}$ [e.Å^{-3}]	0.471	0.366	0.368	0.582
$(\Delta/\rho)_{min}$ [e.Å^{-3}]	- 0.226	−0.344	−0.365	−0.735

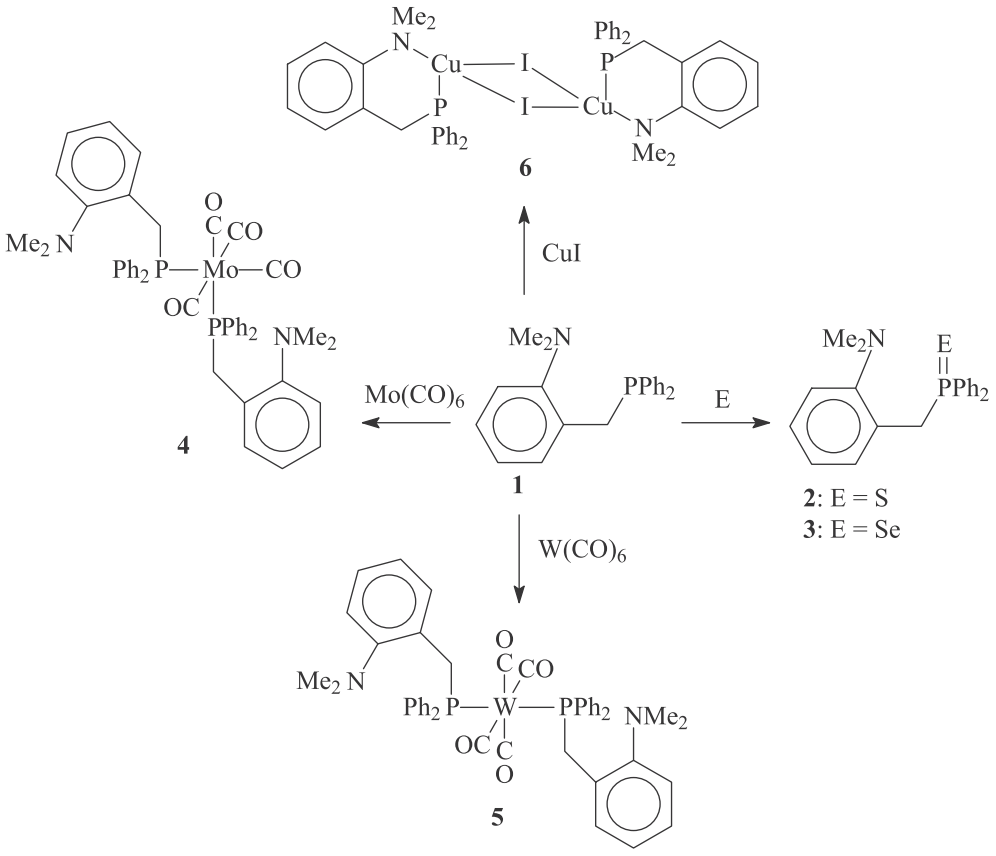

Scheme 1. Preparation of **2**–**6**.

much slower than is intramolecular binding of a second P donor under the reaction conditions employed. Further studies are in progress to investigate the coordination chemistry of ligand **1**. The ^{13}C NMR spectra of the carbonyl ligands in **4** show two signals (209.8 and 216.4 ppm) due to the carbonyls oriented *trans* and *cis* to phosphorus atoms. In contrast, the four carbonyl ligands in **5** are equivalent and gave one signal at 203.4 ppm, typical of the two phosphorus ligands being *trans* to each other. Consistent with these results, The IR spectra in the carbonyl region of **4** show two peaks at 2021 cm^{-1} and doublet type band at 1900 and 1867 cm^{-1}, while in **5** only one doublet type band at 1874 and 1903 cm^{-1} was observable for the four equivalent carbonyl ligands and within the expected value range on comparison to similar *cis*- and *trans*-disubsituted complexes [23]. The IR spectrum of **1**–**6** shows bands in the range of 1431–1437 cm^{-1} due to υ(P–Ph) stretching [24]. Also, the P═S double bond in **2** exhibits vibrations around 650 cm^{-1}, whereas band at around 526 cm^{-1} that is characteristic of P═Se double bond is observed in **3** [25].

The ^{31}P NMR spectrum of **1** shows a single resonance at $\delta = -9.46$ ppm, while the ^{31}P NMR signals of **2**–**6** appear as a singlet at $\delta = 44.79$ ppm (**2**), $\delta = 34.93$ ppm (**3**), $\delta = 34.96$ ppm (**4**), $\delta = 22.08$ ppm (**5**) and $\delta = 32.87$ ppm (**6**), i.e. shifted downfield in comparison with the parent organic ligand **1**, and a move to lower chemical shifts is observed with the decreasing electronegativity of the chalcogen from sulfur to selenium.

The ^{31}P NMR signal of **3** is flanked by two ^{77}Se-satellites with $^{1}J_{Se-P}$ coupling constant of 725.7 Hz. The ^{77}Se NMR spectrum of **3** shows a doublet at $\delta = -286.6$ ppm and the value of coupling constant ($^{1}J_{Se-P} = 729.6$ Hz) match the difference value between the two ^{77}Se-satellites in the ^{31}P NMR spectrum of **3**. Moreover, the ^{31}P NMR signal of **5** is flanked by two ^{183}W-satellites with $^{1}J_{W-P}$ coupling constant of 278.6 Hz.

3.3. Molecular structures of *1*, *2*, *4*, and *6*

Crystals of ***1***, ***2***, ***4***, *and* ***6*** were obtained as described in the experimental section. Compounds ***1***, ***2***, ***4***, *and* ***6*** crystallize in the monoclinic space group $P2_1/c$, monoclinic space group $P2_1/n$, triclinic space group $P\bar{1}$, and monoclinic space group $P2_1$, respectively. The molecular structures of ***1***, ***2***, ***4***, *and* ***6*** are depicted in Fig. 1–4, respectively.

Selected bond distances [Å] and angles [°] **1a**: C(1)–N(1) 1.468(2); C(2)–N(1) 1.458(3); C(3)–N(1) 1.431(2); C(9)–P(1) 1.8562(19); C(10)–P(1) 1.833(2); C(16)–P(1) 1.837(2); C(4)-C(3)-N(1) 121.95(17); C(8)-C(3)-N(1) 119.57(16); C(8)-C(9)-P(1) 112.33(13); C(11)-C(10)-P(1) 125.82(15); C(15)-C(10)-P(1) 116.75(17); C(21)-C(16)-P(1) 118.07(16); C(17)-C(16)-P(1) 123.86(16); C(10)-P(1)-C(16) 101.09(8); C(10)-P(1)-C(9) 101.66(9); C(16)-P(1)-C(9) 102.26(9); C(3)-N(1)-C(2) 114.13(16); C(3)-N(1)-C(1) 115.09(17); C(2)-N(1)-C(1) 109.84(18).

Selected bond distances [Å] and angles [°] **1b**: C(22)–N(2) 1.464(3); C(23)–N(2) 1.463(2); C(24)–N(2) 1.428(2); C(30)–P(2) 1.8560(18); C(31)–P(2) 1.836(2); C(37)–P(2) 1.832(2); C(25)-C(24)-N(2) 121.91(16); C(29)-C(24)-N(2) 119.44(17); C(29)-C(30)-P(2) 112.48(13); C(32)-C(31)-P(2) 118.51(17); C(36)-C(31)-P(2) 123.97(15); C(42)-C(37)-P(2) 125.58(15); C(38)-C(37)-P(2) 116.83(1; C(37)-P(2)-C(31) 98.87(8); C(37)-P(2)-C(30) 102.59(9); C(31)-P(2)-C(30) 103.00(9); C(24)-N(2)-C(23) 115.23(17); C(24)-N(2)-C(22) 113.51(15); C(23)-N(2)-C(22) 110.24(17).

Selected bond distances [Å] and angles [°] **2**: S(1)–P(1) 1.9591(6); P(1)–C(10) 1.8110(17); P(1)–C(16) 1.8122(17); P(1)–C(9) 1.8298(16); N(1)–C(3) 1.429(2); N(1)–C(1) 1.459(3); N(1)–C(2) 1.461(2); C(10)-P(1)-C(16) 103.52(7); C(10)-P(1)-C(9) 105.85(8);

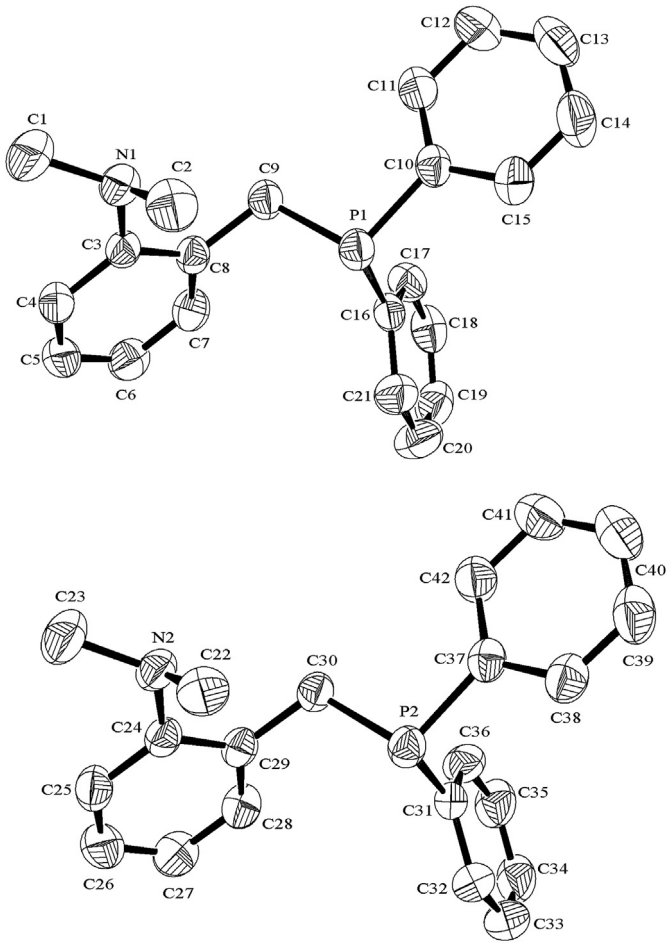

Fig. 1. Molecular structure of the two independent molecules **1a** (above) and **1b** (down) (hydrogen atoms are omitted for clarity).

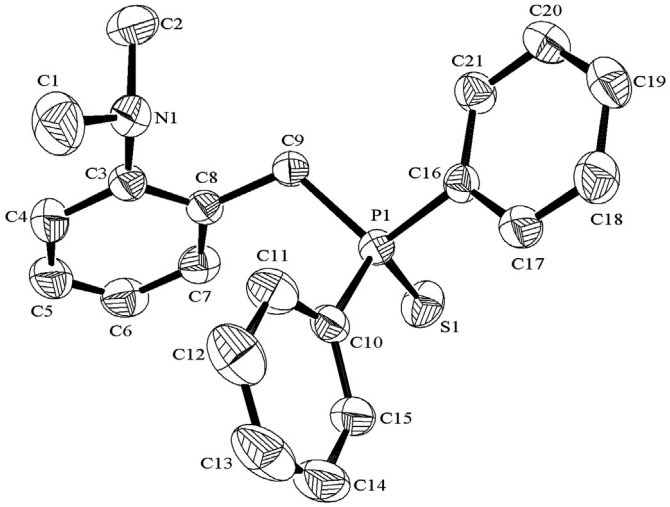

Fig. 2. Molecular structure of **2** (hydrogen atoms are omitted for clarity).

C(16)-P(1)-C(9)104.57(7); C(10)-P(1)-S(1) 114.12(6); C(16)-P(1)-S(1) 112.61(6); C(9)-P(1)-S(1) 115.06(6); C(3)-N(1)-C(1) 114.98(16); C(3)-N(1)-C(2) 112.91(16); C(1)-N(1)-C(2) 111.20(18).

Selected bond distances [Å] and angles [°] **4**: Mo(01)—C(46) 1.975(3); Mo(01)—C(44) 1.985(3); Mo(01)—C(43) 2.034(3); Mo(01)—C(45) 2.041(3); Mo(01)—P(1) 2.5471(7); Mo(01)—P(2) 2.5897(6); P(1)—C(16) 1.827(3); P(1)—C(10) 1.828(2); P(1)—C(9) 1.858(2); P(2)—C(31) 1.837(3); P(2)—C(37) 1.839(3); P(2)—C(30) 1.856(2); O(1)—C(43) 1.137(3); O(2)—C(44) 1.147(3); O(3)—C(45) 1.143(3); O(4)—C(46) 1.146(3); N(1)—C(3) 1.427(5); N(1)—C(1) 1.455(5); N(1)—C(2) 1.467(5); N(2)—C(22) 1.435(4); N(2)—C(24) 1.435(4); N(2)—C(23) 1.449(4); C(46)-Mo(01)-C(44) 87.55(11); C(46)-Mo(01)-C(43) 85.01(11); C(44)-Mo(01)-C(43) 92.34(11); C(46)-Mo(01)-C(45) 85.57(12); C(44)-Mo(01)-C(45) 87.43(11); C(43)-Mo(01)-C(45) 170.57(11); C(46)-Mo(01)-P(1) 86.15(8); C(44)-Mo(01)-P(1) 173.30(7); C(43)-Mo(01)-P(1) 89.39(7); C(45)-Mo(01)-P(1) 89.80(8); C(46)-Mo(01)-P(2)174.68(8); C(44)-Mo(01)-P(2) 88.86(7); C(43)-Mo(01)-P(2) 99.07(7); C(45)-Mo(01)-P(2) 90.35(8); P(1)-Mo(01)-P(2) 97.27(2); C(16)-P(1)-C(10) 105.57(12); C(16)-P(1)-C(9) 101.68(12); C(10)-P(1)-C(9) 105.88(12); C(16)-P(1)-Mo(01) 121.99(8); C(10)-P(1)-Mo(01) 110.14(8); C(9)-P(1)-Mo(01) 110.27(9); C(31)-P(2)-C(37) 104.48(13); C(31)-P(2)-C(30) 102.50(11); C(37)-P(2)-C(30) 103.22(12); C(31)-P(2)-Mo(01) 122.99(9); C(37)-P(2)-Mo(01) 112.64(8); C(30)-P(2)-Mo(01) 108.92(8); C(3)-N(1)-C(1) 114.2(3); C(3)-N(1)-C(2) 115.4(4); C(1)-N(1)-C(2) 112.4(4); C(22)-N(2)-C(24) 112.6(3); C(22)-N(2)-C(23) 111.5(3); C(24)-N(2)-C(23) 115.8(3); O(1)-C(43)-Mo(01) 173.9(2); O(2)-C(44)-Mo(01) 176.0(2); O(3)-C(45)-Mo(01) 173.1(3); O(4)-C(46)-Mo(01) 178.1(3).

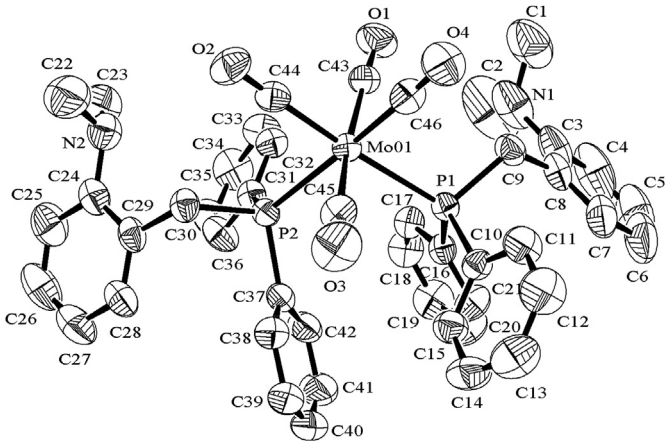

Fig. 3. Molecular structure of **4** (hydrogen atoms are omitted for clarity).

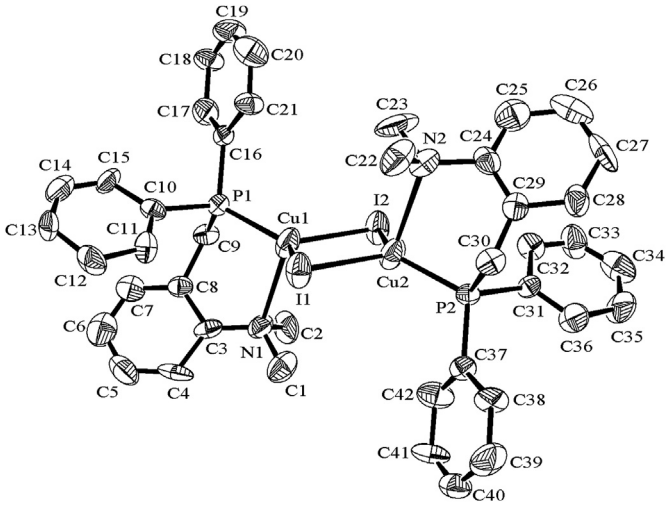

Fig. 4. Molecular structure of **6** (hydrogen atoms are omitted for clarity).

Selected bond distances [Å] and angles [°] **6**: Cu(1)—P(1)

2.199(4); Cu(1)–I(1) 2.575(3); Cu(1)–I(2) 2.596(2); Cu(1)–Cu(2) 2.9274(7); Cu(2)–P(2) 2.202(4); Cu(2)–I(2) 2.579(3); Cu(2)–I(1) 2.589(2); P(1)–C(9) 1.818(16); P(1)–C(16) 1.825(14); P(1)–C(10) 1.830(14); P(2)–C(37) 1.795(14); P(2)–C(31) 1.820(12); P(2)–C(30) 1.876(14); P(1)-Cu(1)-I(1) 124.59(14); P(1)-Cu(1)-I(2) 119.26(14); I(1)-Cu(1)-I(2) 110.96(7); P(1)-Cu(1)-Cu(2) 158.75(13); I(1)-Cu(1)-Cu(2) 55.69(4); I(2)-Cu(1)-Cu(2) 55.27(6); P(2)-Cu(2)-I(2) 124.28(14); P(2)-Cu(2)-I(1) 119.42(14); I(2)-Cu(2)-I(1) 111.07(8); P(2)-Cu(2)-Cu(1) 158.65(12); I(2)-Cu(2)-Cu(1) 55.83(4); I(1)-Cu(2)-Cu(1) 55.23(6); Cu(1)-I(1)-Cu(2) 69.08(7); Cu(2)-I(2)-Cu(1) 68.90(7); C(9)-P(1)-C(16) 106.8(6); C(9)-P(1)-C(10) 101.5(6); C(16)-P(1)-C(10) 101.8(6) C(9)-P(1)-Cu(1) 109.1(5); C(16)-P(1)-Cu(1) 116.3(5); C(10)-P(1)-Cu(1) 119.9(5); C(37)-P(2)-C(31) 104.2(6); C(37)-P(2)-C(30) 107.2(7); C(31)-P(2)-C(30) 101.6(6); C(37)-P(2)-Cu(2) 115.8(5); C(31)-P(2)-Cu(2) 118.7(4); C(30)-P(2)-Cu(2) 108.0(5); C(3)-N(1)-C(1) 116.7(12); C(3)-N(1)-C(2) 105.6(11); C(1)-N(1)-C(2) 107.2(11); C(22)-N(2)-C(24) 118.1(13); C(22)-N(2)-C(23) 111.3(12); C(24)-N(2)-C(23) 113.1(12).

The X-ray structure of **1** contains two crystallographically independent molecules, **1a** and **1b** (Fig. 1), in the asymmetric unit. The molecular structures of **1a** and **1b** show pyramidal geometry about the phosphorus atoms with the C–P–C angles ranging from 98.87(8) – 103.00(9)°.

The molecular structure of **2** shows a distorted tetrahedral geometry about the phosphorus atom with S–P–C and C–P–C angles ranging from 103.52(7)–115.06(6)°. The P═S [1.9591(6) Å] bond length in **2** is similar to those observed for [2-(Me_2NCH_2)C_6H_4]$_3$P(S) [1.962(2) Å] and [2-(Me_2NCH_2)C_6H_4]$_2$PhP(S) [1.9547(10) Å] (**8**) [26].

The crystal structure of **4** (Fig. 3) shows a distorted octahedral environment around the Mo-metal surrounded by four terminal CO ligands and two phosphorus atoms of the two *cis*-oriented *P,N*-ligands with two types of carbonyl ligands have different Mo–C bond distances.

The carbonyl groups *cis* to the phosphorus atoms of the *P,N*-ligands are bound at 2.034(3) Å and 2.041(3) Å, while the other two carbonyl groups are closer to the metal center at distances of 1.975(3) Å and 1.985(3) Å**.** The two Mo–P bond distances [2.5471(7) and 2.5897(6) Å] in **4** are relatively similar. The steric interaction of the two *P,N*-ligands has affected the dimensions of the Mo(CO)$_4$ portion of the molecule. The P(l)-Mo-P(2) angle of 97.27(2)° is largely expanded from the right angle of 90°, while the C(46)-Mo-C(43) angle of 85.01 (11)° is a significantly smaller than the ideal angle of 90° and greater distortion involving the carbonyl groups CO(2) and CO(3). The C(46)-Mo-P(1) angle of 86.15(8)° and the C(44)-Mo-P(2) angle of 88.86(7)° are representative of the tilting of the O(1)-Mo-O(3) axial with respect to the P(1), P(2), Mo, C(46), C(44) plane.

The Mo–P bond distances and the P(l)-Mo-P(2) bond angle in **4** are larger than those found in similar *cis*-[Mo(CO)$_4${PPh$_2$NH$_2$}$_2$] [*Av.* Mo–P: 2.526 Å; P–Mo–P: 90.06(2)°] [27], *cis*-[Mo(CO)$_4${PPh$_2$NH-Bu^t}$_2$] [*Av.* Mo–P: 2.545 Å; P–Mo–P: 95.44(3)°] [28] and *cis*-[Mo(CO)$_4${Ph,PCH$_2$NHC$_6$H$_5$Me-4}$_2$] [*Av.* Mo–P: 2.546 Å; P–Mo–P: 94.2(1)°] [29] complexes.

As in solution, **6** forms a centrosymmetric dimer in the solid state (Fig. 4) in which the central four-membered Cu_2I_2 ring is planar with smaller Cu–I–Cu [69.08(7) and 68.90(7)°] and larger I–Cu–I [110.96(7) and 111.07(8)°] bond angles. Due to the presence of an inversion center, only the anti isomer is observed in the solid state. The Cu–I–Cu angles in **6** are larger than those in [{$Ph_2P(C_6H_4CH_2NMe_2$-*o*)}(CuI)]$_2$ [*Av.* 67.01(2)°], while the situation is reversed for the I–Cu–I angles. Apparently, the presences of the NMe2 groups increase the Cu–I–Cu bond angle, presumably as a result of steric effects. The *anti* arrangement of the two NMe_2 methyl groups with respect to the Cu_2I_2 core in **6** is similar to the *anti* alignment of the two NMe_2 methyl groups with respect to the Cu_2I_2 core in [{$Ph_2P(C_6H_4CH_2NMe_2$-*o*)}(CuI)]$_2$ [30] and differs from The *syn* arrangement of the two NMe_2 methyl groups in [{$Ph_2P(C_6H_4NMe_2$-*o*)}(CuI)]$_2$ [31]. However, in the latter**,** the Cu–I [*Av.* 2.618 Å] bonds are smaller than those of **6** [*Av.* 2.660 Å]**.**

The X-ray crystal structure determination shows a distorted tetrahedral environment of the four-coordinate Cu atoms. The tetrahedral distortion of the environment of the Cu atoms in **6** can be attributed to repulsion between the dimethylamino and phenyl groups.

3.4. Antibacterial activities

The ligand (**1**) and its metal derivatives **4, 5** and **6** were screened for their antibacterial activities using disc diffusion method. Imipenem was used as standard antibiotic which had been compared with the activities of the complexes. Imipenem had an excellent activity against both Gram-positive and Gram-negative bacteria. As shown in Table 2, complexes **4**, **5** and **6** showed more potent antibacterial activity against Gram positive bacteria than the free ligand **1**. This variation can be attributed to combined effect of metal atom and the ligand, which enhances the diffusion of metal complexes as a whole through the lipid layers of cell membrane and/or binding to the protein synthesizing enzyme thus restrained the protein synthesis for bacterial growth of microorganism [32].

All complexes showed almost the same activity against Gram negative bacteria which may be attributed to the nature of the cell wall of the Gram negative bacteria. Complexes **4** and **6** had more antibacterial potential than complex **5** against Gram positive bacteria. *Staphylococcus aureus* was resistant to ligand **1** and complex **5**, and susceptible to complexes **4** and **6**. The highest susceptibility was observed for the *Bacillus subtilis* in the case of using complex **6**, with an inhibition zone of 20 mm, which indicates that this complex could be used as growth control of this bacterium. Compared with the standard antibiotic, all complexes showed overall good activity against *Salmonella typhi* suggesting that these complexes can be used for controlling the growth of this pathogen.

4. Conclusion

In conclusion, we have successfully synthesized ligand **1** (2-PPh_2CH_2-1-$NMe_2C_6H_4$), and their derivatives 2-(E)PPh_2CH_2-1-

Table 2
Antibacterial activity (inhibition zones, mm) of ligand 1 and its metal derivatives 4–6 (1 mg/ml concentration) against selected bacteria.

Compound	Bacteria			
	Bacillus subtilis	*Staphylococcus aureus*	*Escherichia coli*	*Salmonella typhi*
1	10	NA	16	20
4	20	15	18	20
5	13	NA	16	19
6	23	15	18	20
Imipenem	25	24	26	23

Values are the average diameters of the inhibition zones (mm). NA: No Activity observed.

$NMe_2C_6H_4$ (E = S (**2**), Se (**3**)), *cis*-[$Mo(CO)_4$(**1**)] (**4**), *trans*-[$W(CO)_4$(**1**)] (**5**) and [CuI(**1**)]$_2$ (**6**). The ligand behaves as κP-coordination mode rather than $\overset{2}{\kappa}P,N$-mode due to reaction condition, and may be obtained if the reaction is carried out at higher temperatures and for longer time. Further studies are in progress to investigate the coordination of ligand **1**. For **1**, **2**, **4** and **6** the molecular structures are determined. Based on the antibacterial results, we conclude that all compounds **1** and **4**–**6** were good antibacterial agents against both Gram positive and Gram negative bacteria. Complexes **4** and **6** present the highest antibacterial activity and can be considered as promising antimicrobial agents.

Declaration of competing interest

The author declare that there is no conflict of interest.

Acknowledgments

I would like to thank the Deanship of Scientific Research at Al al-Bayt University\ Jordan for funding (grant number 8635/2017). I would also like to thank Prof. Munther khanfor, Dr. Taghleb and Dr. Ziad for their help and support. The X-ray of compounds **1**, **2**, **4** and **6** were provided by Homdi Mango Research center (HMRC), Jordan University, Jordan.

Appendix A. Supplementary data

Supplementary data to this article can be found online at https://doi.org/10.1016/j.jorganchem.2019.121021.

References

[1] a) P.C. Ford, L. Laverman, Coord. Chem. Rev. 249 (2005) 391–403;
b) P. Espinet, K. Soulantica, Coord. Chem. Rev. 193–195 (1999) 499–556;
c) E. Lindner, S. Pautz, M. Haustein, Coord. Chem. Rev. 155 (1996) 145–162;
d) G.R. Newkome, Chem. Rev. 93 (1993) 2067–2089;
e) A. Bader, E. Lindner, Coord. Chem. Rev. 108 (1991) 27–35;
f) S. Maggini, Coord. Chem. Rev. 253 (2009) 1793–1832;
g) J.A. Lemire, J.J. Harrison, R.J. Turner, Nat. Rev. Microbiol. 11 (2013) 371–384.
[2] L.J. Hounjet, R. McDonald, M.J. Ferguson, M. Cowie, Inorg. Chem. 50 (2011) 5361–5378.
[3] P. Suomalainen, S. Jääskeläinen, M. Haukka, R.H. Laitinen, J. Pursiainen, T.A. Pakkanen, Eur. J. Inorg. Chem. (2000) 2607–22613.
[4] J. Andrieu, P. Richard, J. Camus, R. Poli, Inorg. Chem. 41 (2002) 3876–3885.
[5] T.B. Rauchfuss, D.M. Roundhill, J. Am. Chem. Soc. 96 (1974) 3098–3105.
[6] J. Andrieu, J. Camus, P. Richard, R. Poli, L. Gonsalvi, F. Vizza, M. Peruzzini, Eur. J. Inorg. Chem. (2006) 51–61.
[7] D.M. Roundhill, R.A. Bechtold, S.G.N. Roundhill, Inorg. Chem. 19 (1980) 284–289.
[8] T.B. Rauchfuss, J.L. Cements, S.F. Agnew, D.M. Roundhill, Inorg. Chem. 16 (1977) 775–778.
[9] X. Yu, B.O. Patrick, B.R. James, Organometallics 25 (2006) 4870–4877.
[10] D.A. Cavarzan, F.R. Caetano, L.L. Romualdo, F.B. do Nascimento, A.A. Batista, J. Ellena, A. Barison, M.P. de Araujo, Inorg. Chem. Commun. 9 (2006) 1247–1250.
[11] J. Schroer, L.V.P. da Cunha, A.A. Batista, V.M. Deflon, U. Abram, Polyhedron 34 (2012) 108–113.
[12] L.J. Hounjet, M. Bierenstiel, M.J. Ferguson, R. McDonald, M. Cowie, Inorg. Chem. 49 (2010) 4288–4300.
[13] L. Crociani, G. Bandoli, A. Dolmella, M. Basato, B. Corain, Eur. J. Inorg. Chem. (1998) 1811–1820.
[14] D. Hedden, D.M. Roundhill, Inorg. Chem. 24 (1985) 4152–4158.
[15] F. Tisato, F. Refosco, C. Bolzati, A. Cagnolini, S. Gatto, G. Bandoli, J. Chem. Soc., Dalton Trans. (1997) 1421–1427.
[16] L. Dahlenburg, K. Herbst, H. Berke, J. Organomet. Chem. 585 (1999) 225–233.
[17] H.T. Al-Masri, J. Sieler, P. Lönnecke, S. Blaurock, K. Domasevitch, E. Hey-Hawkins, Tetrahedron 60 (2004) 333–339.
[18] a) H.T. Al-Masri, J. Sieler, E. Hey-Hawkins, Appl. Organomet. Chem. 17 (2003) 63–67;
b) H.T. Al-Masri, J. Sieler, E. Hey-Hawkins, Appl. Organomet. Chem. 17 (2003) 641–646;
c) H.T. Al-Masri, J. Sieler, P. Lönnecke, P.C. Junk, E. Hey-Hawkins, Inorg. Chem. 43 (2004) 7162–7169;
d) H.T. Al-Masri, J. Sieler, P.C. Junk, K. Domasevitch, E. Hey-Hawkins, J. Organomet. Chem. 690 (2005) 469–476;
e) H.T. Al-Masri, J. Sieler, S. Blaurock, P. Lönnecke, P. Junk, E. Hey-Hawkins, Z. Anorg. Allg. Chem. 631 (2005) 518–523;
f) H.T. Al-Masri, J. Baldamus, E. Hey-Hawkins, Polyhedron 28 (2009) 3515–3518.
[19] D.D. Perrin, W.L.F. Armarego, Purification of Laboratory Chemicals, third ed., Pergamon, New York, 1988.
[20] O.V. Dolomanov, L.J. Bourhis, R.J. Gildea, J.A.K. Howard, H. Puschmann, J. Appl. Crystallogr. 42 (2009) 339–341.
[21] G.M. Sheldrick, Sheldrick, Acta Crystallogr. A71 (2015) 3–8.
[22] a) J. Andrieu, P. Richard, J.M. Camus, R. Poli, Inorg. Chem. 41 (15) (2002) 3876–3885;
b) T.B. Rauchfuss, F.T. Patino, D.M. Roundhill, Inorg. Chem. 14 (1975) 652–656.
[23] S. Priya, M.S. Balakrishna, J.T. Mague, J. Organomet. Chem. 679 (2003) 116–124.
[24] A. Karacar, M. Freytag, H. Thönnessen, J. Ömelanczuk, P.G. Jones, R. Bartsch, R. Schmeltzer, Heteroat. Chem. 12 (2001) 102–113.
[25] L. Hirsivaara, M. Haukka, S. Jääskeläinen, R.H. Laitinen, E. Niskanen, T.A. Pakkanen, J. Pursiainen, J. Organomet. Chem. 579 (1999) 45–52.
[26] A. Rotar, A. Covaci, A. Pop, A. Silvestru, Rev. Roum. Chim. 55 (11–12) (2010) 823–829.
[27] G.M. Gray, Y. Zhang, J. Crystallogr. Spectrosc. Res. 23 (1993) 711–717.
[28] O. Kühl, S. Blaurock, J. Sieler, E. Hey-Hawkins, Polyhedron 20 (2001) 111–117.
[29] D.L. Davies, F.I. Healey, J. Howarth, D.R. Russell, L.J.S. Sherry, J. Organomet. Chem. 376 (1989) C31–C34.
[30] G.S. Ananthnag, N. Edukondalu, J.T. Mague, M.S. Balakrishna, Polyhedron 62 (2013) 203–207.
[31] M.J. Leitl, F.-R. Küchle, H.A. Mayer, L. Wesemann, H. Yersin, J. Phys. Chem. A 117 (46) (2013) 11823–11836.
[32] R.A. Sanchez-Delgado, K. Lazardi, L. Rincon, J.A. Urbina, J. Med. Chem. 36 (1993) 2041–2043.